ISGSR2007 First International Symposium on Geotechnical Safety & Risk
Oct. 18~19, 2007 Shanghai
Tongji University, China

Displacement scenarios at site scale of rainfall-controlled slow moving active slides in stiff clays

M. Calvello, L. Cascini, G.M. Grimaldi
University of Salerno, Fisciano (SA), Italy

ABSTRACT: A mixed model is proposed to compute displacement scenarios of a slide moving along pre-existing slip surfaces from rainfall scenarios. The model comprises a physically-based transient groundwater analysis of the slope and a kinematic model relating the rate of movement and the inverse of the local factor of safety in critical points along the slip surfaces. The model is calibrated and validated with reference to a well-monitored active slide in stiff clays in Central Italy. The groundwater regime of the critical section of the landslide is computed by means of a transient analysis of the pore water pressures in the slope. The local kinematic model employs a relationship between the velocity of the slide and the shear stress level acting along the slip surface that, in turn, is a function of the time-dependent pore pressures computed by the transient groundwater analysis. The model is defined as "local" in that the analysis is carried out with reference to the stress state at a single point, P_{slip}, on the slip surface. Once calibrated and validated, the model is used as a predictive tool to evaluate displacements scenarios from three rainfall scenarios based on almost 20 years of continuous rainfall measures and representative, respectively, of a year of extremely intense rainfall, of a year of average rainfall, and of a year of minimal rainfall. Although the reliability of the predicted displacement scenarios is not probabilistically evaluated, the three scenarios may be seen as representative, respectively, of an upper boundary, an average estimate and a lower boundary of future displacements.

1 INTRODUCTION

Within the framework of landslide risk theory (Fell et al. 2005), landslide hazard analysis necessarily needs to explicitly take into account the intensity of the analyzed landslide. In the literature, different criteria have been presented to define the intensity of a landslide. Fell (1994) defines the intensity in terms of volume, Cruden and Varnes (1996) define the intensity in terms of velocity. Cascini et al. (2005) underline that the intensity should be based on simple parameters describing the destructiveness of landslides. Among these the maximum movement velocity is a widely accepted parameter, although many others may be also considered suitable for the purpose: total displacement, differential displacement, depth of moving mass, depth of deposited mass, depth of erosion, peak discharge per unit width, kinetic energy per unit area, maximum thrust, impact pressure. In this work, the intensity of landslides in stiff clays is assumed to be equivalent to the mean yearly velocity coupled with the volume of the landslide.

Monitoring data from different rainfall-controlled active landslides in stiff clays indicate that these landslides are generally included in the lower 3 classes of the 1996 classification by Cruden and Varnes (from slow to extremely slow phenomena). Occasional reactivations, however, may yield higher peak velocities than the ones referring to the cyclic seasonal activity of the landslide. Peak velocities up to the 5th class of this classification (rapid phenomena) are reported in the literature (Hungr et al., 2001; Hungr et al., 2005).

Different models exist in the literature to compute landslide displacements from rainfall or pore pressure data. Referring to the methodological approach proposed by Cascini & Versace (1986), they may be classified in 3 groups: phenomenological or black-box models, physically based models, and mixed models (defined as a combination of phenomenological and physically based models). Other authors call the first group “local models” and the second group “global models” (Ledesma et al. 2006). Herein, a mixed model is proposed to compute displacement scenarios from rainfall scenarios. The model comprises a physically-based transient groundwater analysis and a phenomenological relationship between rate of movement and inverse of the factor of safety.

2 THE PORTA CASSIA EARTH SLIDE

2.1 Site description and monitoring data

Orvieto is an ancient hilly town in Central Italy resting on a tufaceous slab that overlies an overconsolidated clayey stratum, where numerous landslides systematically occur (Fig.1a). One of the most disastrous landslides occurred on November 1900, after a period of intense rainfall, in the northern flank of the hill. The technical authority in charge of the inspection of the landslide, reported that the displaced soil mass extended over the whole slope from the rock cliff up to border of the Paglia River plain (Vinassa de Regny 1904). Along the hill, lot of damages occurred and the Umbro-Casentinese road and the Rome-Florence railway were interrupted (Fig.1b).

With the aim of collecting data for a quantitative confirmation of the mechanism governing the slope evolution (Tommasi et al. 1997), in 1982 a monitoring station was installed in the central part of the slope (vertical OR in Fig.1b) comprising a 25m-long inclinometer tube, driven for about 4 m into the bedrock and regularly monitored until 2000, and a Casagrande piezometer placed in the stiff clay at a depth of 31 m b.g.s., whose readings were regularly taken only starting from 1988. Owing to the extremely slow rate of displacement of the middle part of the slide, about 20 years of continuous inclinometric readings are available. Successively, in 1996 and in 1998, three more monitoring stations were installed, each one consisting of an inclinometer and two Casagrande piezometers. Vertical OM is located at the head of the slide while the other two, OV and O4, are in the lower part of the slope, downhill relative to OR (Fig.1b).

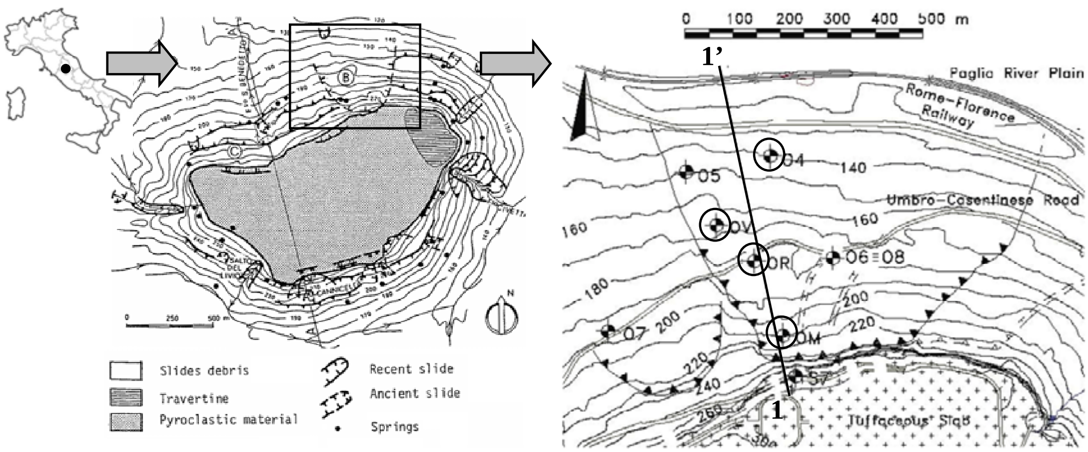

(a) (b)

Fig.1 Map of the Orvieto hill: a) geological map and main landslides, b) instrumented boreholes of the Porta Cassia slide (from Lembo-Fazio et al., 1984; Tommasi et al., 2006)

A section through the Porta Cassia slide, obtained with the aid of the boreholes, shows a three layers stratigraphy (Fig.2a), with a clayey debris upper cover, a middle softened clay layer and a stiff clay bedrock. Fig.2b shows that all the movements affect the first two layers. Particularly inclinometers OR and O4 show a rigid movement of the landslide body on a well defined slip surface, respectively at a depth of 20 meters and 7 meters below ground surface. On the contrary, inclinometers OM and OV show a mass creep profile, in accordance with the hypothesis that the landslide body has a retrogressive style upward and is advancing in the lower part of the slide (Fig.2b) forming new slip surfaces. The groundwater monitoring system along the section comprises one piezometer in the lower bedrock layer, OR, two piezometers in the softened clay, OM and OV, respectively installed at 4,5 and 6 m below ground surface (b.g.s.), and one piezometer in the upper cover, O4, installed at a depth of 6 m b.g.s..

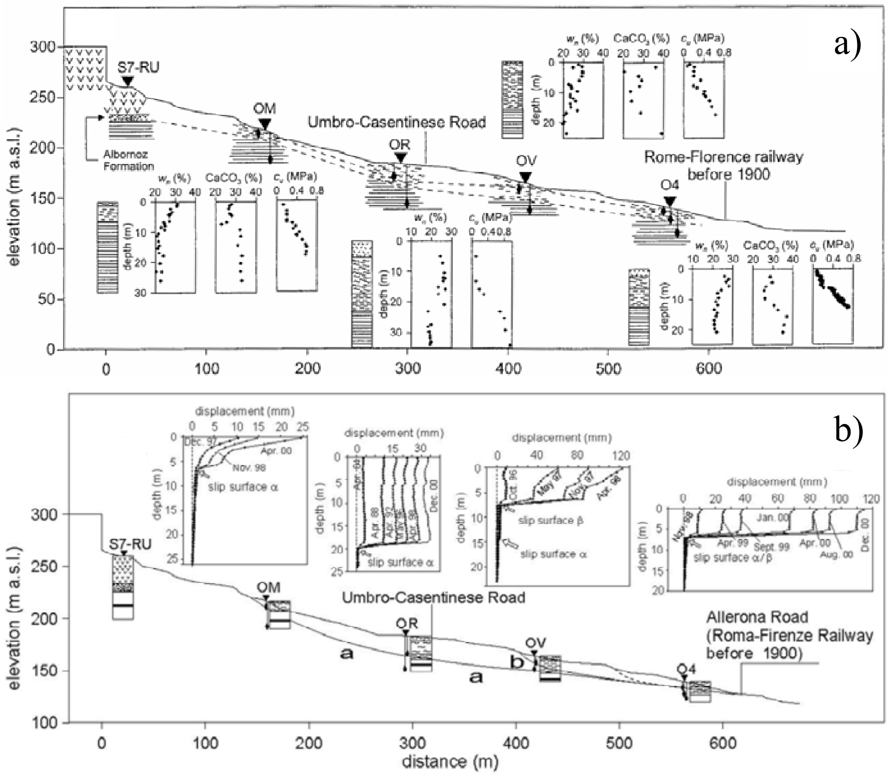

Fig.2 Geotechnical section 1-1' of the Porta Cassia slide: a) logs of physical-mechanical properties and piezometers; b) inclinometric displacements (from Tommasi et al., 2006)

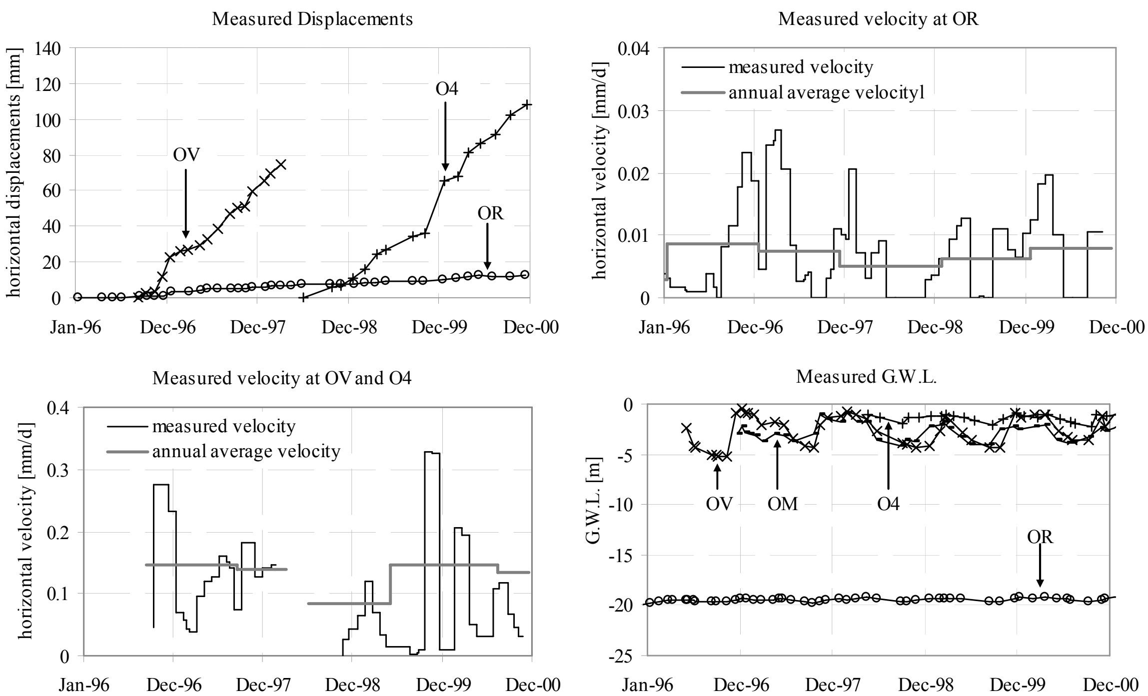

Fig.3 Monitoring field data of the Porta Cassia slide: measured piezometric levels, displacements and velocities (modified from Tommasi et al., 2006; Cafaro et al., 2005)

Fig.3 summarises the available field data, relative to both cumulative displacements for inclinometers OR, OV, O4 and measured groundwater levels for piezometers OM, OR, OV, O4.

The data refer to 5 years of measures between 1996 and 2000 (Tommasi et al. 2006). It is important to underline that the cumulative displacements measured with the inclinometers OR and O4 refer to the deep slip surface (indicated with a in Fig.2b), whereas those in OV refer to a shallower slip surface (indicated with b in Fig.2b). Fig.3 shows how the velocities of the slide along the two slip surfaces, computed from the measured displacements, differ by about one order of magnitude. As for the measured groundwater levels, the three superficial piezometers exhibit similar absolute values and comparable seasonal variations of the order of 3-4 meters, while the deeper one shows both a lower measured water level and lower seasonal differences.

2.2 Landslide typology and activity

Among the landslides' classification systems proposed in the literature, three of them are considered within this work. The first one (Varnes 1978) differentiates landslides on the basis of type of movement and type of material. The second one (Cruden & Varnes 1996) allows a kinematic description of the landslide based on its velocity and its state, distribution and style of activity. The third one (Leroueil et al. 1996) defines four stages of activity and differentiates the type of material in 9 classes. As for the activity of landslides, it is worth highlighting that the definition of "active" landslide proposed by Leroueil et al. (1996) is different from the definition proposed by Cruden & Varnes (1996). According to the classification system by Cruden & Varnes (1996), which in turn refers to the one proposed by the WP/WLI (1993), a landslide is considered active if is currently moving, whereas it is defined as suspended if it has moved within the last year and dormant if its last activity is "older than 1 year". On the contrary, Leroueil et al. (1996) refer to a scheme initially proposed by Vaunat et al. (1994), which considers that a landslide undergoes, during its life, four stages: the pre-failure stage, the failure stage, the post-failure stage and the reactivation stage. Within the latter stage, controlled by localized shear and creep along pre-existing slip surfaces, a phenomenon is defined as active if there is a moving landslide body. No reference is made to time and/or the duration of the movement. Taking into account the displacements measured by the inclinometers, Fig.4 shows how the Porta Cassia landslide can be classified according to the three above-mentioned classification systems.

From Varnes (1978)

TYPE OF MOVEMENT		TYPE OF MATERIAL		
		BEDROCK	ENGINEERING SOILS	
			Predominantly coarse	Predominantly fine
FALLS		Rock fall	Debris fall	Earth fall
TOPPLES		Rock topple	Debris topple	Earth topple
SLIDES	ROTATIONAL	Rock slide	Debris slide	Earth slide
	TRANSLATIONAL			
LATERAL SPREADS		Rock spread	Debris spread	Earth spread
FLOWS		Rock flow (deep creep)	Debris flow (soil creep)	Earth flow (soil creep)
COMPLEX		Combination of two or more principal types of movement		

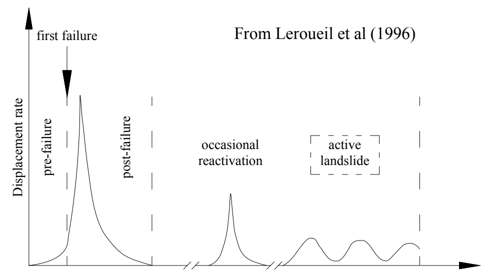

From Cruden & Varnes (1996)

Velocity Class	Description	Velocity (mm/sec)	Typical Velocity
7	Extremely Rapid	5? 0e3	5 m/sec
6	Very Rapid	5? 0e1	3 m/min
5	Rapid	5? 0e-1	1,8 m/hr
4	Moderate	5? 0e-3	1,3 m/mon
3	Slow	5? 0e-5	1,6 m/yr
2	Very Slow	5? 0e-7	15 mm/yr
1	Extremely Slow		

Activity		
State	Distribution	Style
Active	Avancing	Complex
Reactivated	Retrogressive	Composite
Suspended	Widening	Multiple
Inactive	Enlarging	Succesive
Dormant	Confined	Single
Abandoned	Diminishing	
Stabilised	Moving	
Relict		

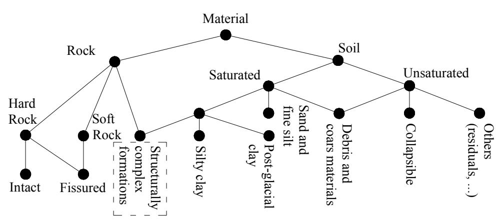

Fig.4 The Porta Cassia landslide according to the classification systems proposed by Varnes (1978), Cruden & Varnes (1996) and Leroueil et al. (1996)

Within the scheme proposed by Varnes (1978), the landslide is a roto-translational slide in earth material. However, if the maximum measured velocity is considered (Cruden & Varnes 1996) the Porta Cassia landslide must be divided in two different phenomena: an extremely slow deep movement (as recorded by inclinometer OR) and a very slow shallower landslide at the toe of the slide (as recorded by inclinometer O4). The deep movement and the shallow one are classified, respectively, as extremely slow and very slow movements (see figures 3c and 3d). According to the same classification system, the slide can be considered retrogressive upward to the tuff slab (as shown by the creep style of the inclinometer profile of location OM) and active. By considering the Leroueil et al. (1996) classification system, the Porta Cassia landslide can be defined as an active slide in a structurally complex formation. Independently from the adopted classification system, the stages of activity of the landslide are strictly related to the time-dependent changes of the groundwater pressures within the slope. When groundwater levels increase the slide starts to move or, if it is already moving, it accelerates; when the groundwater levels decrease the slide decelerates or, eventually, stops moving.

3 MODEL DESCRIPTION

3.1 Groundwater model

Fig.5 shows the Finite Element section considered for the transient analysis of the pore water pressures of the Porta Cassia landslide. The model section refers to the slope section 1-1' reported in figures 1b and 2. The analysis is performed using the commercial finite element code SEEP/W (GEO-Slope 2004) and is relative to 5 years of observations: from January 1996 to January 2001.

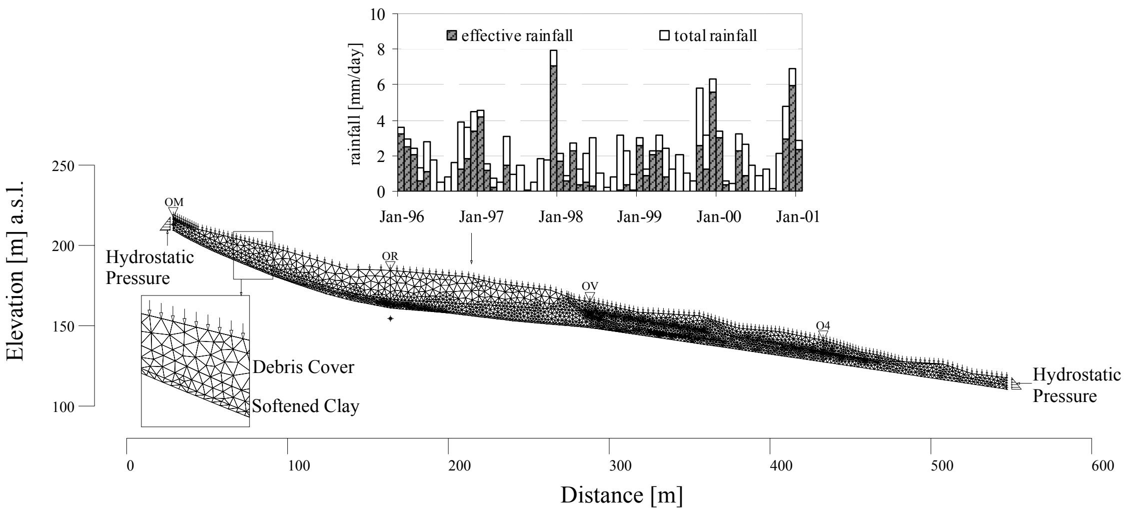

Fig.5 Schematic of the finite element transient groundwater model of the Porta Cassia landslide and rainfall utilized for the transient model

The groundwater model only considers the upper 2 layers of the section (i.e. the debris clayey cover and the softened clay stratum) and assumes that the boundary between the softened clay and the stiff clay bedrock is impermeable. This assumption is in agreement with the water pressures in-situ measurements (Fig.3), which recorded very different groundwater levels between the superficial and deep piezometers both in terms of absolute values and seasonal variations. Moreover it is in accordance with the hydraulic permeabilities of the strata reported by Tommasi et al. (2006), with differences of two orders of magnitude between the values of the upper and lower layer. The results of a preliminary model, which explicitly included the lower bedrock layer, confirm this further by showing that the groundwater regime in the upper two layers does not significantly differ from the groundwater regime relative to the scheme assumed herein. The boundary condition at the ground surface is a unit rate of flow monthly step function equal to the effective monthly rainfall. The other boundary conditions are set by assuming a constant head value on both the left and right boundaries, respectively equal to the elevation of a spring at the top of the slope (OM in Fig.5) and to the mean surface of the Paglia river at the bottom of the slope. The initial conditions are set using the computed pore pressure values of the steady-state analysis with no surface unit flux.

More details about the initial definition of the model, the calibration of the relevant input parameters and the results of the groundwater analysis are reported in Cascini et al. (2008). Herein, a comparison between the pore pressures measured at piezometer O4 and the analogous numerical results is reported (Fig.6) in order to show the reliability of the adopted groundwater model. In fact, although slightly overestimating the maximum groundwater levels reached during periods of intense rainfall, the adopted model is able to reproduce both the magnitude of the groundwater level variation with time and the time-occurrence of the lower and higher peaks.

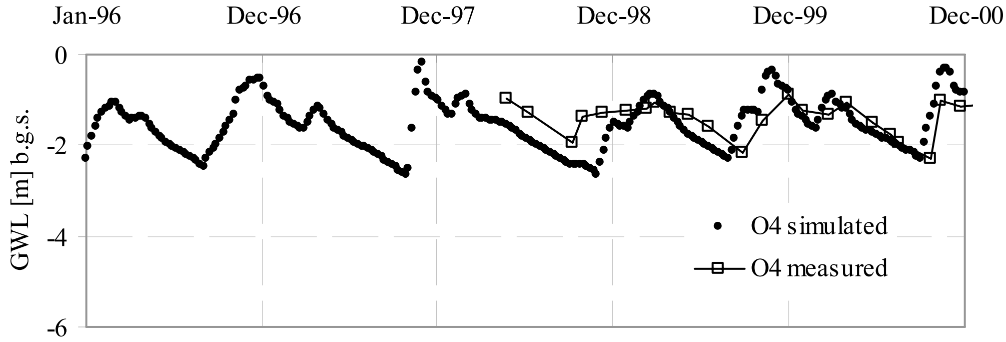

Fig.6 Simulated and measured groundwater level at O4 piezometer

3.2 "Local" kinematic model

The kinematic model, used to compute the time-dependent displacements of the Porta Cassia landslide, employs a phenomenological relationship between the velocity of the slide and the shear stress level acting along the slip surface that, in turn, is a function of the time-dependent pore pressures computed by the transient groundwater analysis. The model is defined as "local" in that the analysis is carried out with reference to the stress state at a single point, P_{slip}, on the slip surface. This point is selected at a depth of 7 m b.g.s., on the monitoring vertical O4, thus referring to the phenomenon at the toe of the slope (see Fig.7). The aim is to analyze the evolution of the fastest recorded movement (Fig.3) and to evaluate the possible correlation of disastrous reactivations, such as the one of 1900, with periods of intense rainfall. Of course, for a complete hazard analysis of the slope, the larger extremely-slow phenomenon, whose movements were recorded by inclinometer OR, should also be considered.

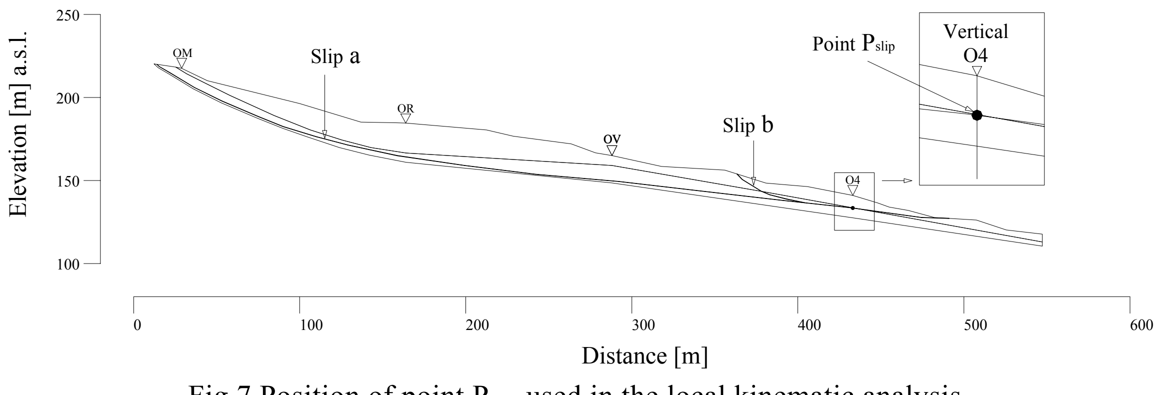

Fig.7 Position of point P_{slip} used in the local kinematic analysis

Referring to inclinometer O4, it was installed during the summer of 1998 and a two-year long period of observations is available: the first readings were taken in November 1998, its last measures refer to December 2000. Along the same vertical a piezometer is installed at a depth of 6 m b.g.s. (Fig.2a). The inclinometric and piezometric data recorded in O4 are reported in Fig.8. With reference to the scheme proposed by D'Elia (1979) and Hutchinson (1988), the inclinometer profiles define three different creep zones: an upper 1.5 meters-thick "superficial predominantly seasonal creep zone", a "mass creep zone" (i.e. shear zone) between 5 and 6 meters b.g.s., and a lower 1 meter-thick "intense creep zone" of basal movement at the bottom of the mass creep. The inclinometric profiles shown in Fig.8a indicate that most of the displacements occur within the deep creep zone. These findings are in accordance with a study on more than 40 slow slides cases by Glastonbury (2006), who found that up to 90% of the total horizontal displacement occur within the deep-creep zone. Fig.8b, which relates the cumulative horizontal displacements to the groundwater level measured in O4, shows that the landslide accelerates as the groundwater rises and slows down when the groundwater level lowers.

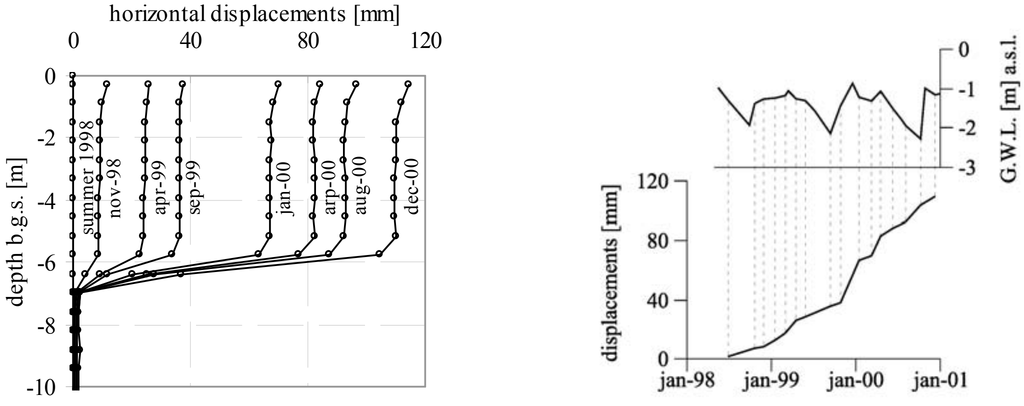

(a) (b)

Fig.8 Monitoring data along vertical O4: a) inclinometric profiles, and b) relationship between measured groundwater levels and cumulative displacements (modified from Tommasi et al., 2006)

The recorded behaviour can be simplified, as shown in Fig.9a, by considering a rigid block moving along a well defined infinitesimal slip surface, at a depth equal to the average depth of the deep creep zone (z_{slip}), which only take into account the creep of that zone and does not account for the relatively small viscous deformation in the mass creep zone nor any superficial seasonal creep deformation. Along the slip surface, the viscous displacements, d_{slip}, can be computed introducing a creep threshold (Yen 1969) above which displacements occur and below which there is no creep. Fig.9b shows the creep threshold considered in this model.

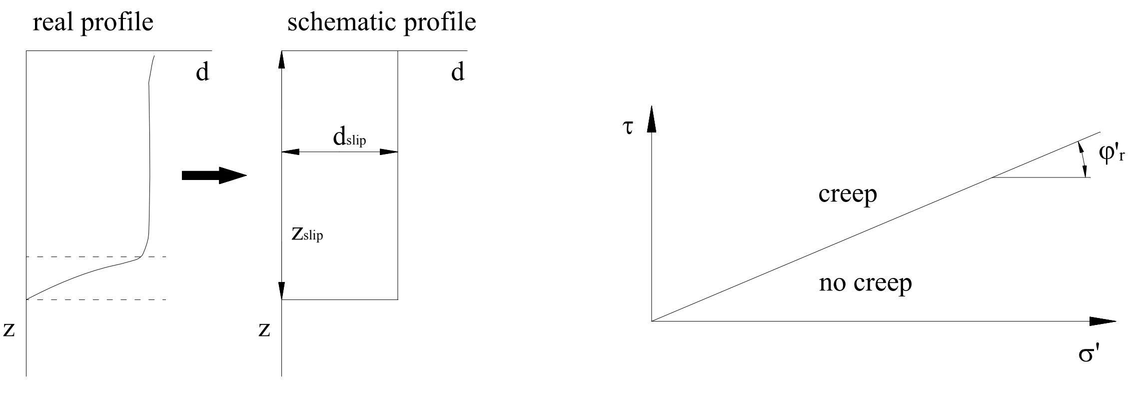

(a) (b)

Fig.9 Simplified creep behaviour adopted in the model: a) profile of horizontal displacements, and b) creep threshold

Given that movements refer to an active slide moving along a pre-existing slip surface, the creep threshold is represented by the residual strength envelope in the Mohr-Coulomb plane:

$$\tau_{creep} = \sigma' \cdot \tan(\varphi'_r) \tag{1}$$

where: τ_{creep} is the shear stress of the creep threshold, σ' is the normal effective stress, φ'_r is the residual friction angle.

The state of stress at the point along the slip surface considered in this model, P_{slip}, is computed using the infinite-slope scheme shown in Fig.10a. Within this scheme, the slip surface is assumed parallel to the ground surface and, assuming that the unit weight of the soil below and above the groundwater surface is about the same, the only component of the local factor of safety varying with time, is $P_w(t)$:

$$\tau_{slip} = \gamma_{sat} \cdot l \cdot \sin\alpha \cdot \cos\alpha \tag{2}$$

$$\sigma_{slip} = \gamma_{sat} \cdot l \cdot \cos^2\alpha \tag{3}$$

$$\sigma'_{slip} = \left(\sigma_{slip} - P_W(t)\right) \tag{4}$$

where: $\gamma_{\sigma\alpha\tau}$ is the saturated unit weight of the soil, l is the depth of the slip surface, α is the slope of the ground surface, $P_w(t)$ is the pore water pressure along the slip surface.

The time-dependent shear stress level at any given point along the slip surface is defined as the ratio of the residual shear strength, $\tau_{creep}(t)$, to the mobilized shear stress, τ_{slip}. The inverse of the shear stress level has the meaning of a local factor of safety, F(t) (Fig.10b):

$$F(t) = \frac{\tau_{creep}(t)}{\tau_{slip}} \tag{5}$$

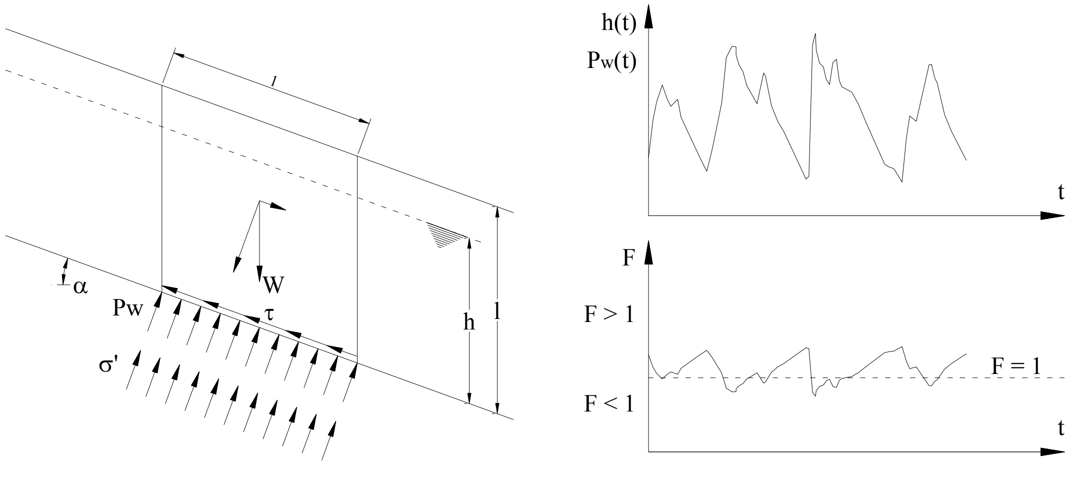

Fig.10 State of stress at the point along the slip surface: a) infinite-slope scheme, b) relationship between the time-dependent water levels and the time-dependent local factor of safety

Finally, the time-dependent creep displacements are computed using a phenomenological relationship, first proposed by Vulliet (1988), between the local factor of safety and the landslide velocity:

$$v_B = B \cdot \left(\frac{1}{F(t)}\right)^n \tag{6}$$

where: B and n are phenomenological constants representing, respectively, the typical velocity of the phenomenon and the variation of viscosity with the excess shear stress (Van Asch et al, 2007).

The displacement monitoring data from inclinometer O4 (Fig.8) were used both for calibrating the input parameters of the model and for validating the results of the calibrated model. Of the two-year long period of observations, only the measures relative to the first year were used for calibrating the model, while the rest of measurements were used to validate it. This is done in order to use some of the observations for evaluating the “predictive ability” of the model. Fig.11 shows the results of the model with reference to both the calibration and the validation phase. The displacement results are obtained integrating the velocity from Eq. (6) over time. The fit between the numerical results and the observations is almost perfect for the calibration phase and remains extremely positive for the validation phase, providing a 0.995 coefficient of correlation for the first phase and a 0.953 for the second. The values of the parameters of the calibrated model are summarised in Table 1.

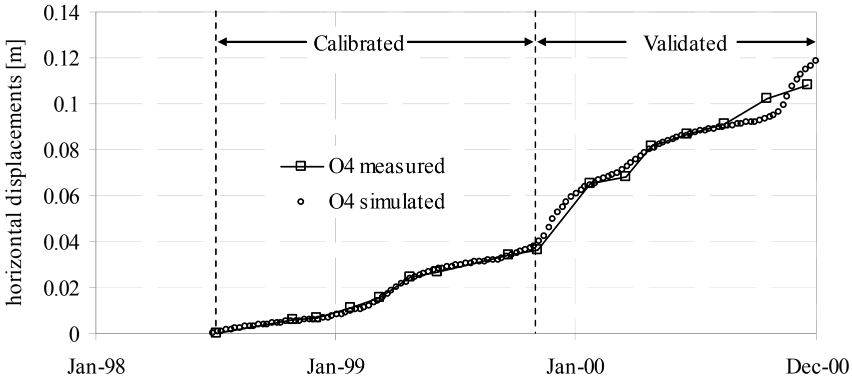

Fig.11 Results of the local kinematic model: comparison between the numerical results and the observations at P_{slip}, a point on the slip surface on the monitoring vertical O4

Table 1 Values of the local kinematic model parameters

l [m]	.	[kN/mc]	’ [°]	B [m/s]	n [-]
7	11	19.7	11.3	1.8 e-6	10

3.3 Slope movements scenarios

Once the groundwater model and the local kinematic model have been calibrated and validated, it is possible to use them as predictive tools to evaluate displacements scenarios from rainfall scenarios (Calvello & Cascini, 2006). Fig.12 shows the three one year-long rainfall scenarios considered for this analysis. All scenarios are based on the investigation of almost 20 years of continuous rainfall measures, from 1981 to 2000. The three scenarios are computed, respectively, using the maximum (scenario 1), average (scenario 2) and minimum (scenario 3) net monthly rainfall recorded during the same month of the year. These scenarios do not originate from a detailed hydrological analysis of the rainfall data, and therefore they do not have a clearly defined probability of occurrence or return period associated with them. Yet they can be considered representative, respectively, of an “extremely unlikely” year of intense rainfall (scen.1), of a year of “average” rainfall (scen.2), an “extremely unlikely” year of minimal rainfall (scen.3).

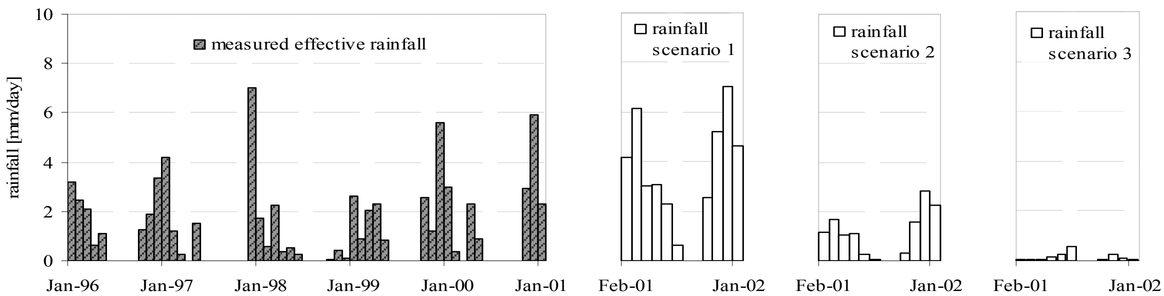

Fig.12 Rainfall scenarios for predictive model: maximum (scenario 1), average (scenario 2) and minimum (scenario 3) net monthly rainfall

Fig.13 shows the horizontal displacements along the slip surface predicted by the model. The reliability of the predicted displacement scenarios cannot be probabilistically evaluated, yet the three scenarios may be seen as representative, respectively, of an upper boundary (scen.1), an average estimate (scen.2) and a lower boundary (scen.3) of future displacements. Of course, this interpretation relies on two assumptions: i) displacements are only caused by changes in groundwater pressures related to rainfall; ii) the transient groundwater regime in the slope is adequately simulated using monthly rainfall data (i.e. the groundwater response to rainfall has a time-lag greater that one month).

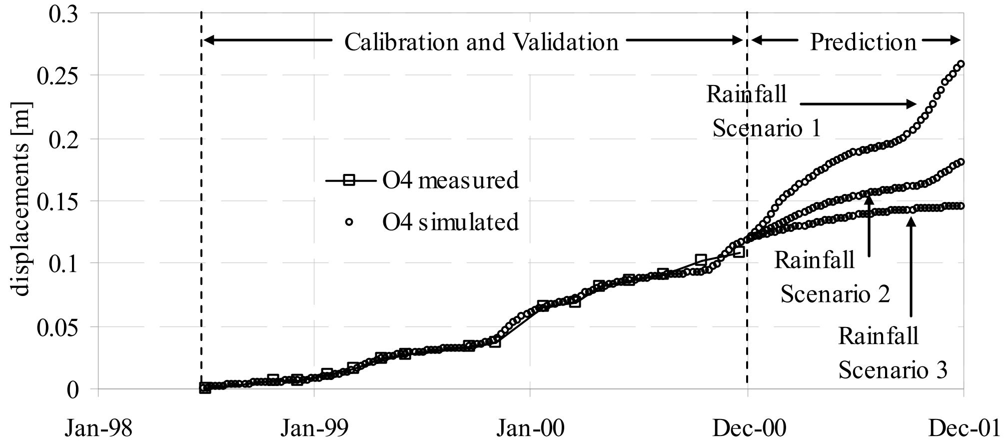

Fig.13 Results of predictive model: displacement scenarios from rainfall scenarios

Within these assumptions, the upper boundary prediction (scenario 1) is particularly relevant in that it allows the evaluation of the maximum velocity and the maximum displacements of the phenomenon. As for the velocity, the mean yearly velocity of the slide can be compared with the thresholds of the classes defined in the classification system by Cruden & Varnes (1996). In this case, the maximum mean yearly velocity observed in O4 was 0.15 mm/d (see Fig.3), the maximum predicted yearly velocity is 0.39 mm/d, and therefore still within the very-slow class. As for the displacements, the value of maximum predicted displacements is about 15 cm, thus more than one order of magnitude lower than the 3 m reported for the 1900 disastrous reactivation of the slide (Tommasi et al. 1997).

4 CONCLUSIONS

Displacement scenarios at site scale of rainfall-controlled slow moving active slides in stiff clays have been computed by means of a numerical model comprising a physically-based transient groundwater analysis of the slope and a phenomenological relationship between the rate of movement of a point along the slip surface and the inverse of the local factor of safety. The results of the model have been evaluated with reference to the Porta Cassia slide, a well-monitored slow-moving active slide in Central Italy.

The displacement results obtained during the calibration and validation phases show the reliability of the proposed model to adequately characterize the evolution of the phenomenon. When the model is used as a predictive tool, three one year-long significant rainfall scenarios have been considered to evaluate three “relevant” displacement scenarios. The upper boundary of future displacements, corresponding to an “extremely unlikely” year of intense rainfall, does not seem to point to extreme rainfall events as the main cause of disastrous reactivations of the slide, such as the one recorded in 1900.

REFERENCES

Cafaro, F., Boldini, D., Tommasi, P. (2005). Drying behaviour of the Orvieto overconsolidated clay. In International Conference on Problematic Soils, Bilsel and Nalbantoglu eds, Famagusta, vol 1, 95-102.

Calvello M., Cascini L. (2006). Predicting Rainfall-induced Movements of Slides in Stiff Clays. Proceedings ECI Conference Geohazards, Lillehammer, Norway, Volume P7, p. 1-8.

Cscini, L., Bonnard, Ch., Corominas, J., Jibson, R., Montero-Olarte, J. (2005). Landslide hazard and risk zoning for urban planning and development. Proceedings of the International Conference on Landslide Risk Management, 31 May - 3 June, Vancouver, Canada, 199-235.

Cascini, L., Calvello, M., Grimaldi, G.M. (2008). Modelling the transient groundwater regime for the displacement analysis of active landslides. Proc. X Int. Symp. on Landslides, Xi'an, China, submitted.

Cascini, L., Versace, P. (1986). Eventi pluviometrici e movimenti franosi. Proceedings XVI Italian Geotechnical Conference, 14-16 May, Bologna, Italy.

Cruden, D.M. & Varnes, D.J. (1996). Landslide types and processes. In: A.K. Turner & R.L. Shuster (Eds.), Landslides: investigation and mitigation. Transportation Research Board, National Research Council, Special Report 247, 36-75. National Academy Press, Washington DC, USA.

D'Elia, B. (1979). Caratteri cinematica delle colate: interventi di stabilizzazione. Rivista Italiana di Geotecnica, Vol. 2, 122-136.

Fell, R. (1994). Landslide risk assessment and acceptable risk. Canadian Geotechnical Journal, 31, pp. 261-272.

Fell, R., Ho, K.K.S., Lacasse, S., Leroi, E. (2005). A framework for landslide risk assessment and management. Proceedings of the International Conference on Landslide Risk Management, 31 May - 3 June, Vancouver, Canada, 3-25.

GEO-SLOPE (2004). Seepage modelling with SEEP/W, User's Guide (version 6.16). GEO-SLOPE International Ltd.; Calgary, Alberta, Canada.

Glastonbury, J., Fell, R. (2006). Deformation Behaviour of Slow-Moving Landslides and Discussion on Characteristics Influencing Their Behaviour. Presentation at the Workshop on the mechanics and velocity of large landslides, 25TH to 28TH September, Courmayeur, Valle d'Aosta, Italy.

Hungr, O., Evans, S.G., Bovis, M., Hutchinson, J.N. (2001). Review of the classification of landslides of the flow type. Environmental and Engineering Geosciences, VII, 221-238.

Hungr, O., Corominas, J., Eherhardt, E. (2005). Estimating landslide motion mechanism, travel distance and velocity. Proceedings of the International Conference on Landslide Risk Management, 31 May - 3 June, Vancouver, Canada, 99-128.

Hutchinson, J.N. (1988). General report: Morphological and geotechnical parameters of landslides in relation to geology and hydrogeology. In Proceedings of the 5th International Symposium on Landslides, Lausanne 10-15 July, 3-35, Balkema, Rotterdam.

Lembo-Fazio, A., Manfredini, G., Ribacchi, R., Sciotti, M. (1984). Slope Failure and Cliff Instability in the Orvieto Hill. In Proceedings of the 4th International Symposium on Landslides, Toronto, Canada 16-21 September, 115-120, Balkema, Rotterdam.

Ledesma, A., Corominas, J., Moya, J., Hürlimann, M., González, D., Brescia, D. (2006). Dynamics of a slow slope movement of a large landslide controlled by rainfall: the case of Vallcebre. Presentation at the Workshop on the mechanics and velocity of large landslides, 25TH to 28TH September, Courmayeur, Valle d'Aosta, Italy.

Leroueil, S., Locat, J., Vaunat, J., Picarelli, L., Lee, H., Faure, R. (1996). Geotechnical characterization of slope movements. Proceedings 7th International Symposium Landslides, Trondheim, June 17-21, 1996, 1, pp. 53-74.

Sassa, K. (1988). Geotechnical model for the motion of landslides. In Proceedings of the 5th International Symposium on Landslides, Lausanne 10-15 July, 37–55, Balkema, Rotterdam.

Tommasi, P., Ribacchi, R., Sciotti, M. (1997). Slow Movements along the slip surface of the 1900 Porta Cassia landslide in the clayey slope of the Orvieto Hill. Rivista Italiana di geotecnica, Vol. 2, pp. 49-58.

Tommasi, P., Pellegrini, P., Boldini, D., Ribacchi, R. (2006). Influence of rainfall regime on hydraulic conditions and movement rates in the overconsolidated clayey slope of the Orvieto hill (central Italy). Canadian geotechnical journal, 43, 70-86.

Varnes, D. J. (1978). Slope movement types and processes. In: Landslide Analysis and Control, in Schuster, R. L., Krizak, eds. Transportation Research Board Special Report No. 176, National Academy of Sciences, Washington, D. C., P. 11-33.

Van Asch, Th.W.J., Van Beek, L.P.H., Bogaard, T.A. (2007). Problems in predicting the mobility of slow-moving landslides. Engineering Geology, 91, 46-55.

Vaunat, J., Leroueil, S., Faure, R. (1994). Slope movements : a geotechnical perspective. Proceedings of the 7th International Congres of the IAEG, Lisbon, 1637-1646.

Vinassa de Regny, P. (1904). Le frane di Orvieto. Giornale di Geologia Pratica, 1, 110-130.

Vulliet, L., Hutter, K. (1988) Viscous-type sliding laws for landslides. Canadian Geotechnical Journal, 25, pp 467-477.

WP/WLI (1993). A suggested method for describing the activity of a landslide. Bulletin of IAEG, 47, 53-57.

Yen, B. C. (1969). Stability of Slopes Undergoing Creep Deformatio., Journal of Soil Mechanics and Foundation Division, American Society of Civil Engineers, 95, SM 4, pp. 1075–1093.